CHINA UNIVERSITY OF PETROLEUM

Xiaohong Chen, Jing Du, Guochang Liu, and Kailong Wu

CUP — TABLE OF CONTENTS

Random noise attenuation using f-x regularized nonstationary autoregression

Guochang Liu[1], *Xiaohong Chen*[1], *Jing Du*[2], *Kailong Wu*[1]

ABSTRACT

We propose a novel method for random noise attenuation in seismic data by applying regularized nonstationary autoregression (RNA) in frequency-space (f-x) domain. The method adaptively predicts the signal with spatial changes in dip or amplitude using f-x RNA. The key idea is to overcome the assumption of linearity and stationarity of the signal in conventional f-x domain prediction technique. The conventional f-x domain prediction technique uses short temporal and spatial analysis windows to cope with the nonstationary of the seismic data. The proposed method does not require windowing strategies in spatial direction. We implement the algorithm by iterated scheme using conjugate gradient method. We constrain the coefficients of nonstationary autoregression (NA) to be smooth along space and frequency in f-x domain. The shaping regularization in least square inversion controls the smoothness of the coefficients of f-x RNA. There are two key parameters in the proposed method: filter length and radius of shaping operator. Synthetic and field data examples demonstrate that, compared with f-x domain and time-space (t-x) domain prediction methods, f-x RNA can be more effective in suppressing random noise and preserving the signals, especially for complex geological structure.

INTRODUCTION

Random noise attenuation in seismic data can be implemented in the frequency-space (f-x) and time-space (t-x) domain using prediction filters (Abma and Claerbout, 1995). Linear prediction filtering assumes that the signal can be described by an autoregressive (AR) model. When the data are contaminated by random noise, the signal is considered to be predicted by the AR filter and the noise is the residual (Bekara and van der Baan, 2009). A number of approaches in f-x domain have been proposed and been used for attenuating random noise. The f-x prediction technique was introduced by Canales (1984) and further developed by Gulunay (1986). The f-x domain prediction technique is also referred as f-x deconvolution by Gulunay (1986). Sacchi and Kuehl (2001) utilized the autoregressive-moving average (ARMA) structure of the signal to estimate a prediction error filter (PEF) and the noise sequence is estimated by self-deconvolving the PEF from the filtered data. Hodgson et al. (2002) presented a novel method of noise attenuation for 3D seismic data, which applies a smoothing filter (e.g. 2D median filter) to each targeted frequency slice and allows targeted filtering of selected parts of the frequency spectrum. The conventional f-x domain prediction uses windowing strategies to avoid that the seismic events are not linear. The data are assumed to be piecewise linear and stationary in an analysis temporal and spatial window. To overcome the potentially low performance of f-x deconvolution that arises with processing structural complex data, Bekara and van der Baan (2009) proposed a new filtering technique for random and coherent noise attenuation in seismic data by applying empirical mode decomposition (EMD) (Huang et al., 1998) on constant-frequency slices in the f-x domain and removing the first intrinsic mode function. In addition, in the research field of seismic data interpolation, Naghizadeh and Sacchi (2009) proposed an adaptive f-x prediction filter, which was used to interpolate waveforms that have spatially variant dips. The f-x domain prediction technique can be implemented in the frequency slice and also in pyramid domain (Sun and Ronen, 1996). The implemented in pyramid domain makes the operators more efficient because one only needs to estimate one prediction filter from many different frequencies (Sun and Ronen, 1996; Hung et al., 2004; Guitton and Claerbout, 2010).

The prediction process can be also achieved in t-x domain (Claerbout, 1992). Abma and Claerbout (1995) discussed f-x and t-x approaches to predict linear events and concluded that f-x prediction is equivalent to t-x prediction with a long time length. Crawley et al. (1999) proposed smooth nonstationary PEFs with micropatches and radial smoothing in the application of seismic interpolation, which typically produces better results than the rectangular patching approach. Izquierdo et al. (2006) proposed a technique for structural noise reduction in ultrasonic nondestructive examination using time-varying prediction filter. Sacchi and Naghizadeh (2009) proposed an algorithm to compute time and space variant prediction filters for noise attenuation, which is implemented by a recursive scheme where the filter is continuously adapted to predict the signal.

Fomel (2009) developed a general method of nonstationary regression with shaping regularization (Fomel, 2007). Shaping regularization has an advantage of a fast iterative convergence. Regularized nonstationary regression (RNA) has been used in multiple subtraction Fomel (2009), time-frequency analysis (Liu et al., 2011b), and nonstationary polynomial fitting (Liu et al., 2011a). Liu and Fomel (2010) introduced an adaptive PEFs using RNA in t-x domain which has been used for trace interpolation.

In this paper, we investigate the f-x domain prediction technique and propose f-x domain RNA to attenuate random noise in seismic data. Firstly, we review the theory of f-x stationary autoregression. Then, we describe the f-x RNA and extend to complex number domain. Next we provide the methodology of random noise attenuation using f-x RNA. Finally, we use synthetic and real data examples to evaluate and compare the proposed method with other noise attenuation techniques, such as f-x domain and t-x domain prediction techniques.

REVIEW OF F-X DOMAIN STATIONARY AUTOREGRESSION

We first consider a seismic section $S(t,x)$ that consists of a single linear event with the slope p and constant amplitude. The frequency domain representation of $S(t,x)$ is given by

$$S(f,x) = A(f)e^{j2\pi fxp}, \tag{1}$$

where $A(f)$is the wavelet spectrum, $f$is the temporal frequency, and $x$is the spatial variable. We assume $x = n\Delta x$, where $n = 1, 2, ..., N$, $N$is the number of traces in the whole section. The relationship between the n-th trace and (n-1)-th trace can be easily shown as

$$S_n(f) = a_1(f)S_{n-1}(f), \tag{2}$$

where $a_1 = \exp(j2\pi fp\Delta x)$. This recursion is a first-order differential equation also known as an AR model of order 1 and represents a single complex-valued harmonic (Bekara and van der Baan, 2009). If there are M linear events in x-t domain, we can have a difference equation of order M (Sacchi and Kuehl, 2001)

$$S_n(f) = \sum_{i=1}^{M} a_i(f)S_{n-i}(f). \tag{3}$$

The recursive filter $\{a_i(f)\}$can be found for predicting a noise-free superposition of complex harmonics. Considering seismic data with additive random noise and non-causal prediction with order $2M$which includes both forward and backward prediction equations (Spitz, 1991; Naghizadeh and Sacchi, 2009), we can obtain

$$\varepsilon_n(f) = S_n(f) - \sum_{i=1}^{M} a_i S_{n-i}(f) - \sum_{i=-1}^{-M} a_i S_{n-i}(f), \tag{4}$$

where $\varepsilon_n(f)$is a complex noise sequence. Canales (1984) argues a causal estimate of signal $\sum_{i=1}^{M} a_i(f)S_{n-i}(f)$ is the predictable part of data obtained by an AR model. This operation is usually called f-x deconvolution (Gulunay, 1986). Noise-free events that are linear in the t-x domain manifest as a superposition of harmonics in the f-x domain and these harmonics can be perfectly predicted using AR filter. If seismic events are not linear, or the amplitudes of wavelet are varying from trace to trace, they no longer follow Canaless assumptions (Canales, 1984). One needs to perform f-x deconvolution over a short sliding window in time and space. This leaves the choice of window parameters (window size and length of overlapping between adjacent windows). Bekara and van der Baan (2009) discuss some limitations of conventional f-x deconvolution in detail.

F-X DOMAIN REGULARIZED NONSTATIONARY AUTOREGRESSION

Nonstationary autoregression has been developed and used in signal processing (Bakrim et al., 1994; AllenAboutajdine et al., 1996; Izquierdo et al., 2006) and seismic data processing (Sacchi and Naghizadeh, 2009). Fomel (2009) developed a general method of nonstationary autoregression using shaping regularization technology and applied it to multiples subtraction. In this paper, we extend the RNA method to f-x domain for complex numbers and apply it to seismic random noise attenuation.

Consider two adjacent seismic traces $S_n(f)$ and $S_{n-1}(f)$ in f-x domain of a seismic section that consists of a single nonlinear event with the slope p_n and varying amplitude $B_n(f)$. Similar to equation 1, we can write

$$[S_n(f) = \frac{B_n(f)}{B_{n-1}(f)} e^{j2\pi f \Delta x p_n} S_{n-1}(f) = a_1(f) S_{n-1}(f). \tag{5}$$

From equation 5 we can find that the coefficients of AR is the function of space index n and frequency index f. Therefore, we can use nonstationary autoregression to describe this problem. Equation 5 describes the relation between two traces. If we consider multiple traces, the nonstationary autoregression can be defined as (Fomel, 2009)

$$\varepsilon_n(f) = S_n(f) - \sum_{i=1}^{M} a_{n,i}(f) S_{n-i}(f), \tag{6}$$

where n and $f$are the coordinate of space and frequency, respectively. If considering the situation of non-causal nonstationary autoregression, we can rewrite the Nonstationary autoregression models (equation 6) as

$$\varepsilon_n(f) = S_n(f) - \sum_{i=1}^{M} a_{n,i}(f) S_{n-i}(f) - \sum_{i=-1}^{-M} a_{n,i}(f) S_{n-i}(f). \tag{7}$$

Equation 7 indicates that one trace noise-free in f-x domain can be estimated by weighted stacking adjacent traces with the weights $a_{n,i}(f)$, which is varying along the space and frequency. Note that the difference between equations 4 and 6 is that the coefficients are varying with space coordinate n in equation 7. To obtain the coefficients $a_{n,i}(f)$ from equation 7, we can transform equation 7 to the following least square problem:

$$\min_{a_{n,k}(f)} ||S_n(f) - \sum_{i=1}^{M} a_{n,i}(f) S_{n-i}(f) - \sum_{i=-1}^{-M} a_{n,i}(f) S_{n-i}(f)||_2^2, \tag{8}$$

where $\|\|_2^2$denotes the squared L-2 norm. Note that both the data $S_n(f)$ and the coefficients $a_{n,i}(f)$ are in complex numbers domain.

The problem of the minimization in equation 7 is ill-posed because it has more unknown variables than constraints. To obtain the spatial-varying coefficients in nonstationary autoregression, several methods can be employed (AllenAboutajdine et al., 1996). Some of these are related to the expansion of the spatial-varying coefficients in terms of a given sets of orthogonal basis functions and estimation of the coefficients of the expansion by the least-square method (Izquierdo et al., 2006). Naghizadeh and Sacchi (2009) used exponentially weighted recursive least square (EWRLS) to solve the adaptive problem and applied it to seismic trace interpolation. Fomel (2009) proposed regularized nonstationary autoregression in which shaping regularization technology (Fomel, 2007) is used to constrain the smoothness of the coefficients of nonstationary autoregression. In this paper, we also adopt shaping regularization to solve the under-constrained problem equation 8.

With the addition of a regularization term, equation 8 can be written as

$$\min_{a_{n,i}f} ||S_n(f) - \sum_{i=-M,i\neq 0}^{M} a_{n,i}(f)S_{n-i}(f)||_2^2 + R[a_{n,i}(f)], \tag{9}$$

where R denotes the shaping regularization operator. Fomel (2009) compared classic Tikhonovs regularization with shaping regularization in RNA problem. Shaping regularization Fomel (2007) provides a particularly convenient method of enforcing smoothness in iterative optimization schemes. Shaping regularization has clear advantages of a more intuitive selection of regularization parameters and a faster iterative convergence (Fomel, 2009). In the shaping regularization, we assume the initial value for the estimated model $a_{n,i}(f)$ is zero. If we choose a more appropriate initial value, we can have a fast iterative convergence of the conjugate-gradient iteration in shaping regularization.

Note that the RNA equation in this paper (equation 9) is in complex number domain while the RNA used in multiples subtraction (Fomel, 2009) is in real number domain. Analogous to RNA in real number domain, we force the complex coefficients $a_{n,i}(f)$ in equation 9 to have a desired behavior, such as smoothness. In shaping regularization technology, we need to choose a shaping operator $\mathbf{S}$ (Fomel, 2007). In this paper, we choose shaping operator $\mathbf{S}$ as Gaussian smoothing with adjustable radius r. Fomel (2007) indicated Gaussian smoothing can be implemented by repeated triangle smoothing operator. Both the data $S_n(f)$ and the coefficients $a_{n,i}(f)$ are complex numbers, but the shaping operator $\mathbf{S}$ is real. Therefore, shaping operator $\mathbf{S}$ is operated in real and imaginary parts of the complex coefficients respectively and the L-2 norm in equation 9 is the norm of complex numbers. When using the algorithm of conjugate-gradient iterative inversion with shaping regularization proposed by Fomel (2007) to solve the complex RNA, we only need to replace transpose of real number by conjugate transpose of complex number.

Once we obtain the complex coefficients of RNA, we can achieve an estimation of signal

$$\tilde{S}_n(f) = \sum_{i=-M, i\neq 0}^{M} a_{n,i}(f) S_{n-i}(f). \tag{10}$$

When we use f-x RNA to noise attenuation, we first select a time window in t-x domain and transform the data to f-x domain. The usage of time window is to guarantee that the data is approximately stationary in time. The f-x NAR can deal with spatial nonstationary data in f-x domain. Then we use equation 9 with shaping regularization to compute the coefficients $a_{n,i}(f)$ and use equation 10 to estimate the signal in f-x domain. Finally, we transform data back to the t-x domain and repeat for the next time window.

The computational cost of the proposed method is $O\left(N_d N_f N_{iter}\right)$, where N_d is data size, $N_f$is filter size, $N_{iter}$is the number of conjugate-gradient iterations. If $N_{iter}$and N_f are small, this is a fast method. In practical implementation, we can choose the range of computed frequency to reduce the computation cost. In addition, if we can simplify the coefficients not to be frequency-dependent, we can apply RNA in frequency slice. In that case the different-frequency slices can be processed in parallel. And the computation cost and memory requirements can be further reduced.

Consider a simple section (Figure 2(a)), which includes one event, 501 traces. The event is obtained by convolution with Ricker wavelet. Both the dip and amplitude of the event are space-varying. The travel time is a sine function and the amplitude of the Ricker wavelet is multiplied by$B(x) = 0.2(x-2.5)^2 + 0.5$. This event is obviously nonstationary in space. We add some random noise to it (Figure 1(b)). The event is greatly contaminated by random noise, especially in the middle part, because the signal of the middle part is poorer than the sideward and the noise levels are the same in the whole section. We use three methods, f-x domain prediction, t-x domain prediction, and f-x domain RNA, to suppress random noise. The f-x domain and t-x domain prediction methods we used in this paper are discussed by (Abma and Claerbout, 1995). The f-x domain prediction is implemented over a sliding window of 20 traces width with 50% overlap and the filter length is 4, $M = 2$ in equation 4 and the t-x domain prediction is implemented over the same sliding window and the filter length in space and time are 4 and 5 respectively. The f-x RNA is implemented with the parameters: the filter length is 4, $M = 2$ in equation 8; the smoothing radiuses in space and frequency axes of shaping regularization are respectively 20 and 3, $r_x = 20$, $r_f = 3$. Comparing the results of f-x RNA (Figure 1(f)) with other prediction methods (Figures 4(c) and 4(d), we find that the f-x RNA is more effective in random noise attenuation for this simple nonstationary data. From the difference sections (Figure 2), we find that all the three methods remove some effective signals. However, the proposed method removes fewest signals than other two methods. Note that the removed signals by t-x and f-x prediction methods are bigger in the sideward part than middle part, because the filters are the same in a sliding time window while the amplitude and slope of the event are different.

In order to quantitatively evaluate the effect of denoising between different meth-

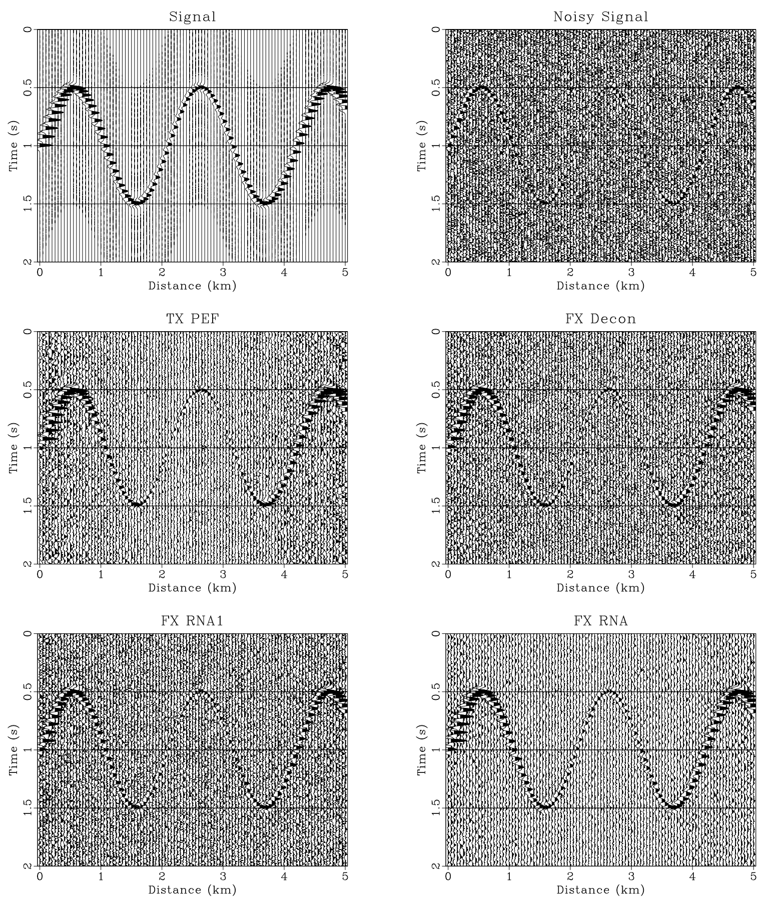

Figure 1: (a) Synthetic data. (b) Noisy data (SNR=1.53). (c) Result of f-x domain prediction (SNR=2.53). (d) Result of t-x domain prediction (SNR=3.12). (e) Result of f-x RNA without constraint of smoothness along the frequency axis (SNR=4.87). (f) Result of f-x RNA with $r_f = 3$ (SNR=5.06). We decimate the data for display purpose. rna2d/simple sin,nsin,tpefpatch,fxpatch,npre1,npre2

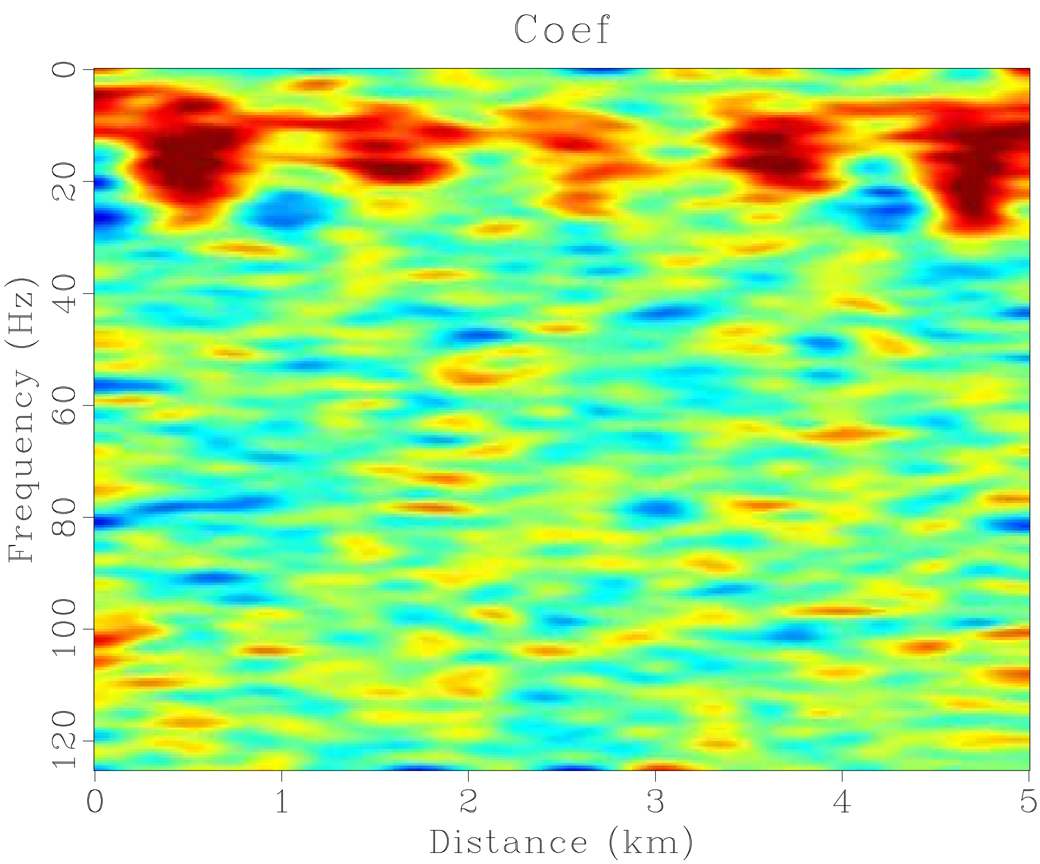

Figure 2: The real part of coefficients at a given shift $a_{n,i=1}(f)$. rna2d/simple npar2

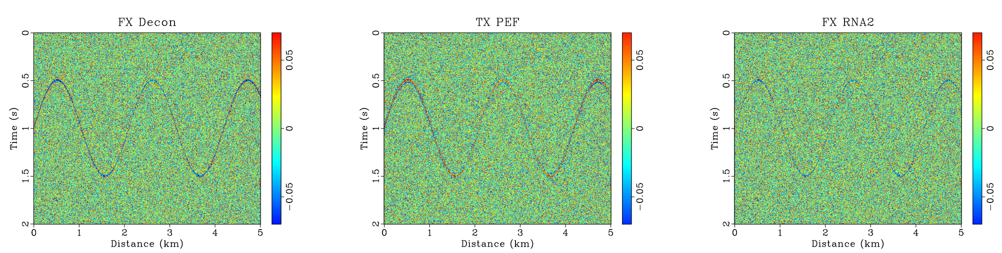

Figure 3: Difference sections of f-x domain prediction (a), t-x domain prediction (b), and f-x RNA (c). rna2d/simple fxdiff,mpapatch,ndiff2

ods, we use signal-to-noise ratio (SNR) to compare these three methods. The SNR is estimated by

$$SNR = 10\log_{10}\left(\frac{\sum\limits_{t,n}\left[d_n(t)\right]^2}{\sum\limits_{t,n}\left[d_n(t)-r_n(t)\right]^2}\right), \tag{11}$$

where $r_n(t)$ is the noisy section and $d_n(t)$is the noisy-free section or the section after noise attenuation. In this simple example, the SNR of the input data without processing is 1.53. After noise attenuation, the SNR of f-x RNA is 5.06 dB, and the SNRs of f-x domain and t-x domain prediction are respectively 2.53 dB and 3.12 dB. The f-x RNA can improve SNR more greatly.

To test the sensitivity to the constraint of smoothness along the frequency axis, we give the result of f-x RNA without constraint of smoothness along the frequency axis in this simple example (Figure 1(e)). The result without constraint along frequency axis (Figure 1(e)) is a little worse than that with constraint along frequency. But both of them are better than the results of conventional f-x domain and t-x domain prediction. Therefore, to reduce the computation cost, we can simplify the coefficients not to be frequency-dependent when the input seismic data is huge. It is a tradeoff between computation cost and effect of noise attenuation.

Because the dip and amplitude of the event are varying smoothly, f-x RNA can predict the signal with smooth coefficients $a_{n,i}(f)$. To specify the coefficients, we display the real parts of the complex coefficients at a given shift $a_{n,i=1}(f)$ (Figure 2). The reason of displaying real parts not imaginary parts is that the signs of real parts of coefficients are the same for forward and backward prediction. We find that the real parts of the complex coefficients are smooth. The smoothing radius controls the smoothness of the coefficients. If we only use one adjacent trace to predict the trace, the coefficients should have the expression

$$a_{n,i=1}(f) = \frac{B_n(f)}{B_{n-1}(f)} e^{j2\pi f\Delta x p_n}. \tag{12}$$

From equation 12 we can note that if the dip and amplitude are smoothly varying, the coefficients are smooth. Therefore, we use Gaussian shaping regularization to constrain the coefficients when solving the least squares equation 9.

EXAMPLES

We demonstrate the effectiveness of the proposed f-x RNA on a synthetic shot gather and a field poststack dataset.

Synthetic shot gather

Figure 4(a) shows a synthetic shot gather with four hyperbolic events, 501 traces. Some random noise is added to this gather. We do not use windows in time for this

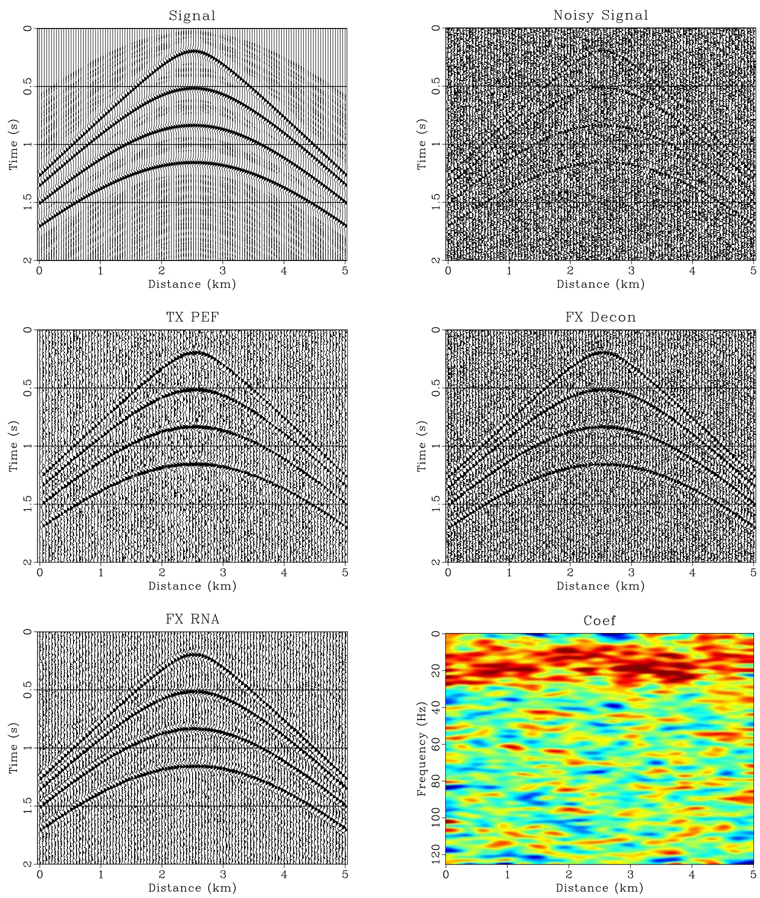

Figure 4: (a) Synthetic shot gather. (b) Noisy gather. (c) Result of f-x domain prediction (SNR=0.98). (d) Result of t-x domain prediction (SNR=1.25). (e) Result of f-x RNA (SNR=3.12). (f) The real part of coefficients at a given shift $a_{n,i=1}(f)$. We decimate the data in (a)-(e) for display purpose. rna2d/shot para,npara,tpefpatch,fxpatch,npre,npar

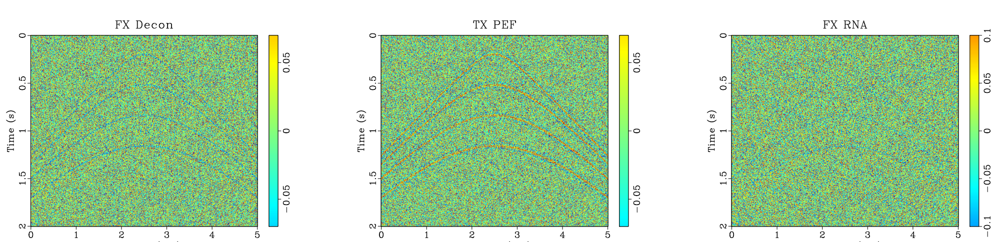

Figure 5: Difference sections of f-x domain prediction (a), t-x domain prediction (b), and f-x RNA (c). rna2d/shot fxdiff,mpapatch,ndiff

example. For f-x RNA, the length of filter is $M = 4$ and the smoothing radiuses in space and frequency axes are respectively 20 and 3, $r_x = 20$, $r_f = 3$. The f-x domain prediction is implemented over a sliding window of 20 traces width with 50% overlap and the filter length is 6, $M = 3$ and the t-x domain prediction is implemented over the same sliding window and the filter length in space and time are 6 and 5 respectively. The estimated nonstationary coefficients by the proposed f-x RNA are shown in Figure 4(f). Note that the middle coefficient is bigger than the sideward, which is because the dip of the middle is smaller than the sideward. The results of three methods are shown in Figures 4(d)- 6(d), respectively. The f-x RNA achieves a similar result to f-x domain and t-x domain prediction methods. However, we use equation 11 to compute the SNRs of the results of three methods. The SNRs of three methods are 0.98 dB, 1.25 dB, 1.67 dB, respectively. The f-x RNA can improve SNR more greatly. The f-x RNA solves the nonstationary case by allowing the coefficients smoothly varying, while f-x domain or t-x domain prediction method uses windowing strategies. From the difference sections (Figure 7(a)- 5(c)), we find that f-x domain and t-x domain prediction methods damage more signals than f-x RNA. If we use windows in time for this example, we can obtain better results. This example shows that f-x RNA can be used for random noise attenuation in shot gather.

Field poststack dataset

Figure 6 is a seismic image from marine data after time migration. The preprocessing, such as bandpass filtering and migration, has removed some noise. However, some noise still exists in this image (indicated by arrows). This dataset is not structurally too complex and the noise seems random. Therefore, we can use t-x domain or f-x domain prediction methods to attenuate the random noise. Figures 6(b)- 6(d) show the results of random noise attenuation using f-x domain prediction, t-x domain prediction and f-x RNA, respectively. The length of time window is 512 ms in all the three methods. For f-x RNA, the filter length is $M = 4$, and the smoothing radiuses in space and frequency axes are respectively 20 and 3, $r_x = 20$, $r_f = 3$. The f-x domain prediction is implemented over a sliding window of 20 traces width with 50% overlap and the filter length is $M = 4$ and the t-x domain prediction is implemented over the same sliding window and the filter length in space and time are 6 and 5 respectively. The f-x domain and t-x domain prediction methods removes random noise well in the case that the events are approximately linear. In the area of complex structure, however, both of the f-x domain and t-x domain prediction methods can not obtain a good result. Compared to f-x domain and t-x domain prediction methods, f-x RNA removes more noise and preserves signals (Figure 7(a)- 7(c)). Note that f-x domain and t-x domain prediction methods remove some signals, especially for complex structure (indicated by arrows in Figures 7(a) and 7(b)). We display the zoomed section in Figure 8(a)- 8(d). The zoomed sections show the proposed method is more effective than other methods, especially in the area of complex structure indicated by arrow. The f-x RNA gives a good result not only for linear events but also for curving events (indicated by arrows in Figure 8(a)- 8(d)).

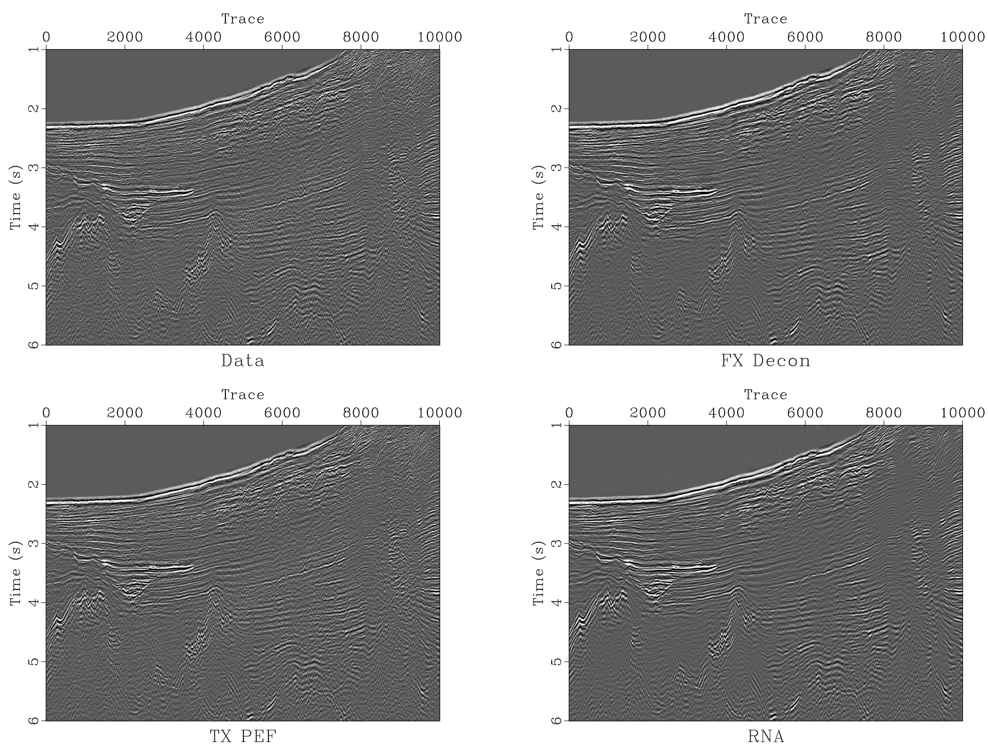

Figure 6: (a) A field marine data set. (b) The result of f-x domain prediction. (c) The result of t-x domain prediction. (d) The result of f-x RNA. rna2d/real data,fxm,tx,npre

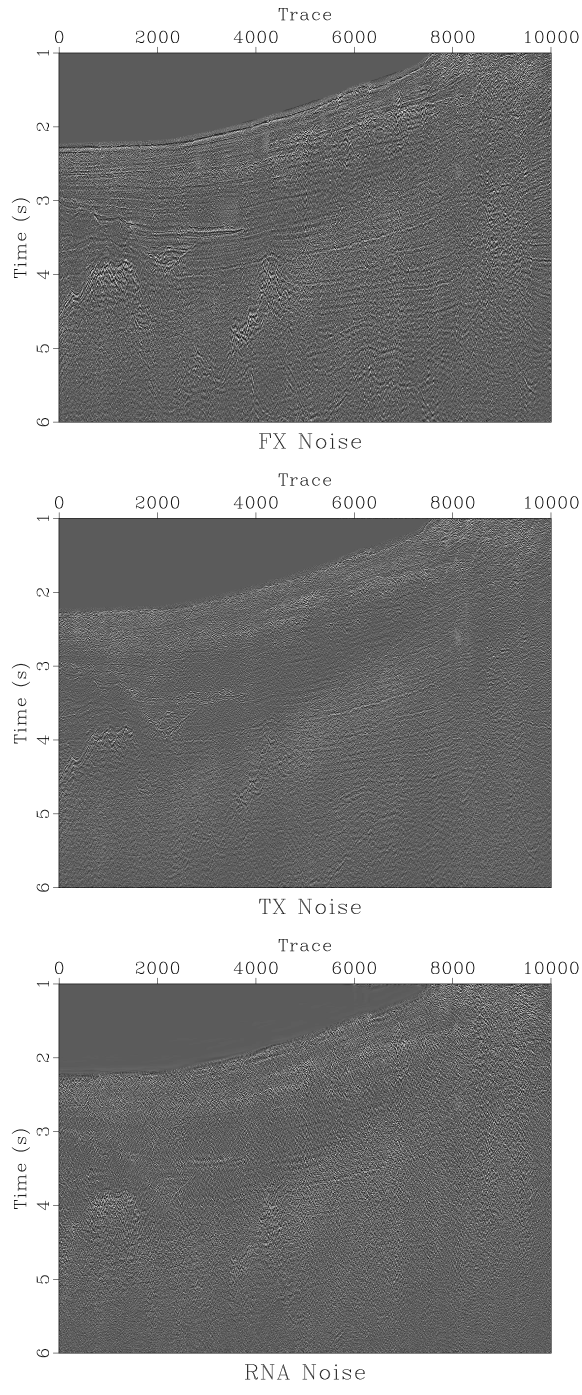

Figure 7: Difference sections of f-x domain prediction (a), t-x domain prediction (b), and f-x RNA (c). rna2d/real fxdiff,txdiff,nprediff

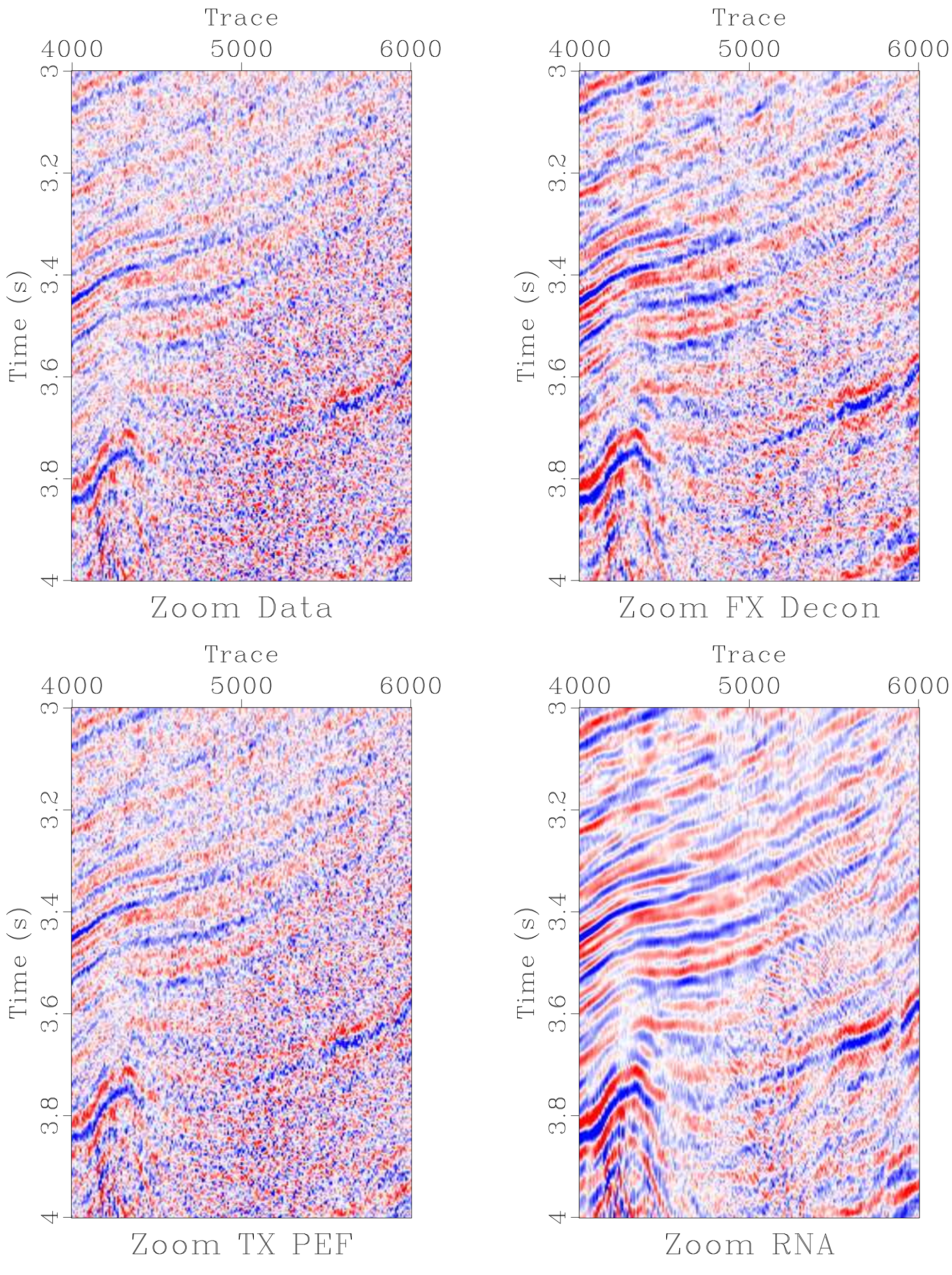

Figure 8: Zoomed sections. (a) Original data. (b) The result of f-x domain prediction. (c) The result of t-x domain prediction. (d) The result of f-x RNA. rna2d/real zdata,zfxm,ztx,znpre

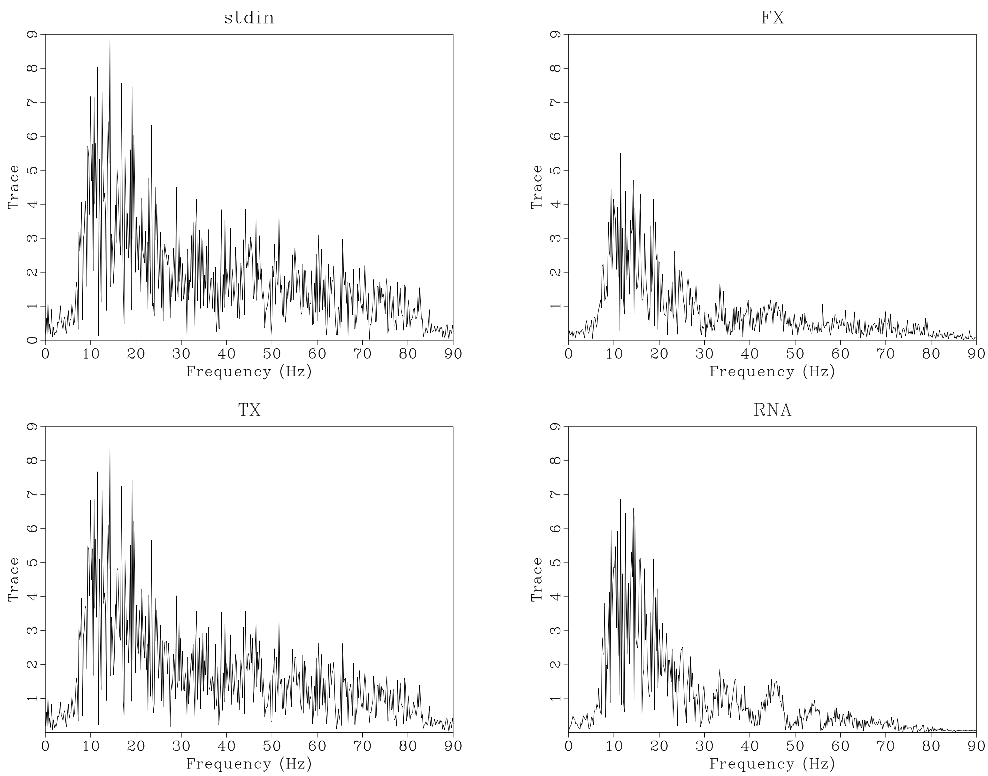

Figure 9: Comparison on spectra of one trace at 6000 m in field marine data (Figure 6- 6(d)). (a)-(d) are the amplitude spectra of one trace at 6000 m in Figures 6- 6(d), respectively. rna2d/real dataf,fxf,txf,npref

From the comparison on the spectra of a trace randomly chosen as shown in Figure 9(a)- 9(d), we can see that f-x domain and t-x domain prediction methods greatly attenuate frequency components in [10,30] Hz, which includes effective signals. Thus, the difference sections of f-x domain and t-x domain prediction methods (Figures 7(a) and 7(b)) include more signals than f-x RNA (Figure 7(c)). For high frequency random noise, all the three methods can achieve a similar result (Figure 9(a)- 9(d)).

CONCLUSIONS

We have proposed a novel method for random noise attenuation using f-x domain regularized nonstationary autoregression. f-x RNA uses shaping regularization to constrain the complex nonstationary coefficients to be smooth along space and frequency axes. Contrary to conventional noise-reduction technology, f-x domain and t-x domain prediction, f-x RNA invokes no piecewise-stationary assumption. The parameters used in f-x RNA are intuitive because the parameters directly control the smoothness of complex coefficients. The proposed method has two key parameters: filter length and smoothing radius of shaping operator. Filter length is related to the number of events and smoothing radius is related to the smoothness of desired RNA complex coefficients. As the smoothing radius increases, the result of RNA approaches the result of stationary autoregression. This approach does not require breaking the input data into local windows along space axis, although it is conceptually analogous to sliding spatial windows with maximum overlap. Both synthetic and field data examples confirm that the proposed approach can be significantly more effective than other noise-reduction methods in improving signal-to-noise ratio and preserving the signals. A comparison with the recently published t-x RNA method has not been attempted, but remains of interest for further investigation. The proposed method is easy to extend to the 3D case (f-x-y domain). One only needs to add a space dimension in the equation 9 when applied in 3D case. Besides random noise attenuation, f-x RNA may have other applications in seismic data processing, such as seismic trace interpolation.

ACKNOWLEDGMENTS

We would like to thank Sergey Fomel, Jingye Li and Yang Liu for inspiring discussions and help with the code in the Madagascar software package. We also thank the associate editor, the reviewer Clement Kostov and one anonymous reviewer for their constructive comments, which improved the quality of the paper. This work is financially supported by Important National Science and Technology Specific Projects of China (grant 2011ZX05023-005-005).

REFERENCES

Abma, R., and J. Claerbout, 1995, Lateral prediction for noise attenuation by t-x and f-x techniques: Geophysics, **60**, 1187–1896.

AllenAboutajdine, D., A. Adib, and A. Meziane, 1996, Fast adaptive algorithms for ar parameters estimation using higher order statistics: IEEE Transactions on Signal Processing, **44**, 1998–2009.

Bakrim, M., D. Aboutajdine, and M. Najim, 1994, New cumulant-based approaches for non-gaussian time varying ar models: Signal Processing, **139**, 107–115.

Bekara, M., and M. van der Baan, 2009, Random and coherent noise attenuation by empirical mode decomposition: Geophysics, **74**, V89–V98.

Canales, L., 1984, Random noise reduction: 54th Annual International Meeting, Soc. of Expl. Geophys., 525–527.

Claerbout, J., 1992, Earth soundings analysis: Processing versus inversion: Blackwell Scientific Publications.

Crawley, S., J. Claerbout, and R. Clapp, 1999, Interpolation with smoothly nonstationary prediction-error filters: 69th Annual International Meeting, Soc. of Expl. Geophys., 11541157.

Fomel, S., 2007, Shaping regularization in geophysical-estimation problems: Geophysics, **72**, R29–R36.

———, 2009, Adaptive multiple subtraction using regularized nonstationary regression: Geophysics, **74**, V25–V33.

Guitton, A., and J. Claerbout, 2010, An algorithm for interpolation in the pyramid domain: Geophysical Prospectin, **58**, 965976.

Gulunay, N., 1986, Fxdecon and complex wiener prediction filter: 56th Annual International Meeting, Soc. of Expl. Geophys., 279–281.

Hodgson, L., D. Whitcombe, S. Lancaster, and P. Lecocq, 2002, Frequency slice filtering - a novel method of seismic noise attenuation: 72nd Annual International Meeting, Soc. of Expl. Geophys., 2214–2218.

Huang, N. E., Z. Shen, S. R. Long, M. L. Wu, H. H. Shih, Q. Zheng, N. C. Yen, C. C. Tung, and H. H. Liu, 1998, The empirical mode decomposition and hilbert spectrum for nonlinear and nonstationary time series analysis: Proc. R. Soc. London A, **454**, 903995.

Hung, B., C. Notfors, and S. Ronen, 2004, Seismic trace interpolation using the pyramid transform: 74th Annual International Meeting, Soc. of Expl. Geophys., 20172020.

Izquierdo, M., M. Hernndez, and J. Anaya, 2006, Time-varying prediction filter for structural noise reduction in ultrasonic nde: Ultrasonics, **44**, e1001–e1005.

Liu, G., X. Chen, J. Li, J. Du, and J. Song, 2011a, Seismic noise attenuation using nonstationary polynomial fitting: Applied Geophysics, **8**, 18–26.

Liu, G., S. Fomel, and X. Chen, 2011b, Time-frequency analysis of seismic data using local attributes: Geophysics, **76**, P23–P34.

Liu, Y., and S. Fomel, 2010, Trace interpolation beyond aliasing using regularized nonstationary autoregression: 80th Annual International Meeting, Soc. of Expl. Geophys., 3662–3666.

Naghizadeh, M., and M. Sacchi, 2009, f-x adaptive seismic-trace interpolation: Geophysics, **74**, V9–V16.

Sacchi, M., and H. Kuehl, 2001, Arma formulation of fx prediction error filters and projection filters: Journal of Seismic Exploration, **9**, 185–197.

Sacchi, M., and M. Naghizadeh, 2009, Adaptive linear prediction filtering for random noise attenuation: 79th Annual International Meeting, Soc. of Expl. Geophys., 3347–3351.

Spitz, S., 1991, Seismic trace interpolation in the f-x domai: Geophysics, **56**, 785794.

Sun, Y., and S. Ronen, 1996, The pyramid transform and its application to signal/noise separation: SEP Annual Report, **93**, 161176.

Noncausal f-x-y regularized nonstationary prediction filtering for random noise attenuation on 3D seismic data

Guochang Liu and Xiaohong Chen

ABSTRACT

Seismic noise attenuation is very important for seismic data analysis and interpretation, especially for 3D seismic data. In this paper, we propose a novel method for 3D seismic random noise attenuation by applying noncausal regularized nonstationary autoregression (NRNA) in f-x-y domain. The proposed method, 3D NRNA (f-x-y domain) is the extended version of 2D NRNA (f-x domain). f-x-y NRNA can adaptively estimate seismic events of which slopes vary in 3D space. The key idea of this paper is to consider that the central trace can be predicted by all around this trace from all directions in 3D seismic cube, while the 2D f-x NRNA just considers the middle trace can be predicted by adjacent traces along one space direction. 3D f-x-y NRNA uses more information from circumjacent traces than 2D f-x NRNA to estimate signals. Shaping regularization technology guarantees the nonstationary autoregression problem can be realizable in mathematics with high computational efficiency. Synthetic and field data examples demonstrate that, compared with f-x NRNA method, f-x-y NRNA can be more effective in suppressing random noise and improve trace-by-trace consistency, which are useful in conjunction with interactive interpretation and auto-picking tools such as automatic event tracking.

INTRODUCTION

Seismic noise attenuation is very important for seismic data processing and interpretation, especially for 3D seismic data. Among the methods of seismic noise attenuation, prediction filtering is one of the most effective and most commonly used methods, e.g., (Gulunay, 1986; Galbraith, 1984; Gulunay et al., 1993; Sacchi and Kuehl, 2001). Prediction filtering can be implemented in f-x domain or $t-x$ domain (Hornbostel, 1991; Abma and Claerbout, 1995). Abma and Claerbout (1995) compared f-x method and $t-x$ method and gave the advantages and disadvantages of both these methods. The proposed method in our paper belongs to the category of f-x domain methods. The f-x prediction technique was introduced for random noise attenuation on 2D poststack data by Canales (1984) and further developed by Gulunay (1986). Wang and West (1991) and Hornbostel (1991) used noncausal filters for random noise attenuation on stacked seismic data and obtain a good result. Linear prediction filtering states that the signal can be described by an autoregressive (AR) model, which means that a superposition of linear events transforms into a superposition of complex sinusoids in the f-x domain. Sacchi and Kuehl (2001) utilized the autoregressive-moving average (ARMA) structure of the signal to estimate a prediction error filter (PEF) and applied ARMA model to attenuate random noise. Liu et al. (2009) applied ARMA-based noncausal spatial prediction filtering to avoid the model inconsistency.

As already noted, these above mentioned f-x methods assume seismic section is composed of a finite number of linear events with constant dip in $t-x$ domain. To cope with the assumption continuous changes dips, short temporal and spatial analysis windows are usually used in f-x prediction filtering. Except using windowing strategy, several nonstationary prediction filters are proposed and used in seismic noise attenuation and interpolation. Naghizadeh and Sacchi (2009) proposed an adaptive f-x prediction filter, which was used to interpolate waveforms that have spatially variant dips. Fomel (2009) developed a general method of regularized nonstationary aoturegression (RNA) with shaping regularization (Fomel, 2007) for time domain inverse problems. Liu et al. (1991) propose a method for random noise attenuation in seismic data by applying noncausal regularized nonstationary autoregression (NRNA) in frequency domain, which is implemented for 2D seismic data. These nonstationary methods can control algorithms adaptability to changes in local dip so that they can process curved events.

If using f-x prediction filter to suppress random noise on 3D seismic data, one need to run the 2D algorithm slice by slice (along inline x or crossline y). To use more information to predict the effective signal in 3D data, several geophysicists extended f-x prediction filtering to 3D case. Chase (1992) designs and applies 2-D prediction filters in the plane defined by the inline and crossline directions for each temporal frequency slice of the 3-D data volume. Ozdemir et al. (1999) applied f-x-y projection filtering to attenuate random noise of seismic data with low poor signal to noise ratio (SNR), in which the crucial step of 2-D spectral factorization is achieved through the causal helical filter. Gulunay (2000) proposed using full-plane noncausal prediction filters to process each frequency slice of the 3-D data. Wang (2002) applied f-x-y 3D prediction filter to implement seismic data interpolation and gave a good result. Hodgson et al. (2002) presented a novel method of noise attenuation for 3D seismic data, which applies a smoothing filter to each targeted frequency slice and allows targeted filtering of selected parts of the frequency spectrum.

In this paper, we extend f-x NRNA method (Liu et al., 1991) to f-x-y case and use f-x-y NRNA to attenuate random noise for 3D seismic data. The coefficients of 3D NRNA method are smooth along two space coordinates (x and y) in f-x-y domain. This paper is organized as follows: First, we provide the theory for random noise on 3D seismic data, paying particular attention to establishment of f-x-y NRNA equations with constraints and implementation of it with shaping regularization. Then we evaluate and compare the proposed method with f-x NRNA using synthetic and real data examples and discuss the parameter selection problem associated with our algorithm.

METHODOLOGY

The review of f-x NRNA

Seismic section $S(t,x)$ in f-x domain is predictable if it only includes linear events in $t-x$ domain. The relationship between the n-th trace and (n-i)-th trace can be easily described as

$$S_n(f) = \sum_{i=1}^{M} a_i(f) S_{n-i}(f), \tag{1}$$

where M is the number of events in 2D seismic section. Eq. (1) describes forward prediction equations, namely causal prediction filtering equations (Gulunay, 2000). In the case of both forward and backward prediction equations (noncausal prediction filter), Eq. 1 can be written as (Spitz, 1991; Gulunay, 2000; Naghizadeh and Sacchi, 2009; Liu et al., 1991)

$$S_n(f) {=} \sum_{i=1}^{M} a_i S_{n-i}(f) {+} \sum_{i=-1}^{-M} a_i S_{n-i}(f), \tag{2}$$

where M is the parameter related to the number of events. Note that Eq. 2 implies the assumption $\sum_{i=1}^{M} a_i S_{n-i}(f){=}0.5S_n(f)and\sum_{i=-1}^{-M} a_i S_{n-i}(f){=}0.5S_n(f)$. Theoretically, $a_i$in forward prediction equations is the complex conjugation of a_{-i}in backward equations (Galbraith, 1984). Gulunay (2000) pointed that it is possible to reduce the order of the normal equations from 2M to M because the coefficients of noncausal prediction filter have conjugate symmetry. f-x prediction filtering has the assumption that the events of seismic section are linear. If seismic events are not linear, or the amplitudes of wavelet are varying, they no longer follow linear or stationary assumptions (Canales, 1984). One needs to perform f-x prediction filtering over a short sliding window in time and space to cope with continuous changes in dips (Naghizadeh and Sacchi, 2009). Fomel (2009) developed a general method of RNA using shaping regularization technology, which is implemented for real number. Liu et al. (1991) extended the RNA method to f-x domain for complex numbers and applied it to seismic random noise attenuation for 2D seismic data. The f-x NRNA is defined as (Liu et al., 1991)

$$\varepsilon_n(f) = S_n(f) - \sum_{i=1}^{M} a_{n,i}(f) S_{n-i}(f) - \sum_{i=-1}^{-M} a_{n,i}(f) S_{n-i}(f). \tag{3}$$

Eq. 3 indicates that one trace noise-free in f-x domain can be predicted by adjacent traces with the different weights $a_{n,i}(f)$. Note that the weights $a_{n,i}(f)$ is varying along the space direction, which indicated by subscript i in $a_{n,i}(f)$. In Eq.

3, the coefficients $a$is the function of space i, but it is not in Eq. 2. When applying f-x NRNA to seismic noise attenuation, we assume the prediction error$\varepsilon_n(f)$ is the random noise and the predictable part $\sum_{i=1}^{M} a_{n,i}(f)S_{n-i}(f) + \sum_{i=-1}^{-M} a_{n,i}(f)S_{n-i}(f)$ is the signal. Finding spatial-varying coefficients $a_{n,i}(f)$ form Eq. 3 is ill-posed problem because there are more unknown variables than constraint equations. To obtain the coefficients, we should add constraint equations. Shaping regularization (Fomel, 2009) can be used to solve the under-constrained problem (Liu et al., 1991). The RNA method can also be used for seismic data processing in t-x-y domain, such as seismic data interpolation (Liu and Fomel, 2011).

f-x-y NRNA for random noise attenuation

Two dimensional f-x NRNA only considers one space coordinate x. If we use f-x NRNA on 3D seismic cube, we usually apply f-x RNA in one space slice. f-x NRNA reduces the effectiveness because the plane event in 3D cube is predictable along different directions rather than only one direction. Therefore, we should develop 3D f-x-y NRNA to suppress random noise for 3D seismic data.

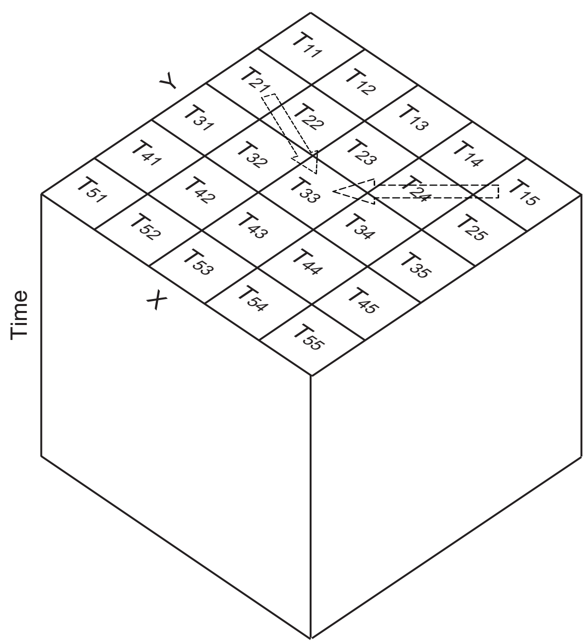

Figure 1: The f-x-y prediction filter. The trace T_{33} is predicted from circumjacent traces $T_{11} \sim T_{55}$(except itself T_{33}). rna3d/. fig1

Next, we use Fig. 1 to illustrate the idea of f-x-y NRNA. The middle trace $T_{33}$is the one we want to predict. Trace T_{33} can be predicted from circumjacent traces $T_{11} \sim T_{55}$(except itself T_{33}). The prediction process includes all different directions. For example, if we use $T_{21}$to predict T_{33}, we can estimate a corresponding coefficient using the described algorithm in the following. f-x-y NRNA uses all around traces to predict the middle trace. Therefore, the prediction uses more information than f-x NRNA. For all the traces in 3D cube, similar to the trace T_{33}, we can use circumjacent traces to predict them. Mathematically, we can write the prediction process as

$$S_{x,y}(f) = \sum_{i=-M,i\neq 0}^{M} a_i(f) S_{x,y,i}(f), \tag{4}$$

where M and i are the number and index of circumjacent traces, respectively. In the case of Fig. 1, M=24 and i is from 1 to 24. Note that $S_{x,y,i}(f)$indicates the 24 circumjacent traces around $S_{x,y}(f)$. Eq. 4 is the equations of noncausal regularized stationary autoregression. Similarly to f-x NRNA, considerng the nonstationary case, we can obtain

$$\tilde{S}_{x,y}(f) = \sum_{i=-M,i\neq 0}^{M} a_{x,y,i}(f) S_{x,y,i}(f), \tag{5}$$

where $a_{x,y,i}(f)$is the space-varying coefficients, which means they have three free degrees, space axis x, space axis y and shift axis i. $\tilde{S}_{x,y}(f)$can be regarded as the estimation of noise-free signal. However, the coefficients $a_{x,y,i}(f)$ are not known. Once we obtain the coefficients, we can estimate the effective signal using Eq. 5 Similar to f-x NRNA, we use shaping regularization to solve this ill-posed problem. Here, we assume that the coefficients $a_{x,y,i}(f)$ f-x-y RNA are smooth along two space axes x and y, which is reasonable because the curved surface event in 3D seismic data is locally plane. Therefore, we can obtain the following least square problem with shaping regularization

$$\min_{a_{x,y,i}(f)} ||S_{x,y}(f) - \sum_{i=-M,i\neq 0}^{M} a_{x,y,i}(f) S_{x,y,i}(f)||_2^2 + R[a_{x,y,i}(f)], \tag{6}$$

where R[.] denotes shaping regularization term which constrains coefficients $a_{x,y,i}(f)$ to be smooth along space axes. We use one coefficient with a given frequency and a given shift (e.g., from T_{21} to T_{33} indicated by arrow in Fig. 1) to explain the constraint in Eq. 6. This 3D cube of coefficient with a given frequency and a given shift can be expressed as $a_{x,y,i_0}(f_0)$, which is smooth along with variables x and y. The smooth constraint of coefficients is the objective of shaping regularization. Finally, we use Eq. 6 to obtain obtain the complex coefficients of f-x-y RNA, and use Eq. 5 to achieve the estimation of signal.

Transform-base methods can also be used for seismic noise attenuation (Ma and Plonka, 2010). Tang and Ma (1991) proposed to total-variation-based curvelet shrinkage for 3D seismic data denoising in order to suppress nonsmooth artifacts caused by the curvelet transform. Because the f-x-y NRNA method uses shaping regularization to solve the ill-posed inverse problem and is complemented in frequency domain, it has higher computation efficiency than curvelet-based methods.

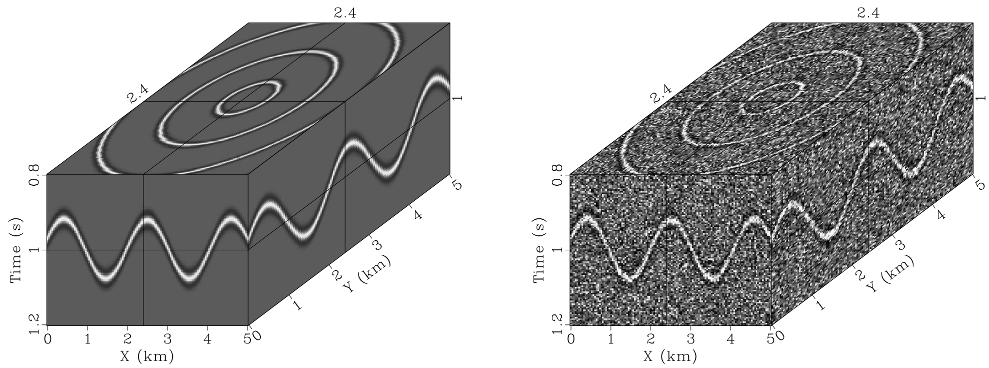

Figure 2: Synthetic benchmark 3D cube with one curved surface event (a) and noisy data cube (b). $\boxed{\text{rna3d/sin sin,cmp}}$

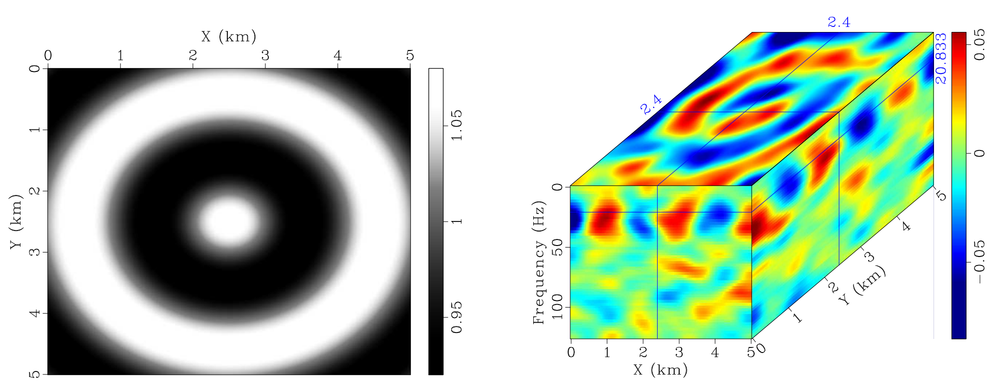

Figure 3: (a) Travel time of the event in Fig. 2(a). (b) The imaginary part of f-x-y NRNA coefficients at a given shift $a_{x,y,i_0}(f)$ $\boxed{\text{rna3d/sin tsin,flt}}$

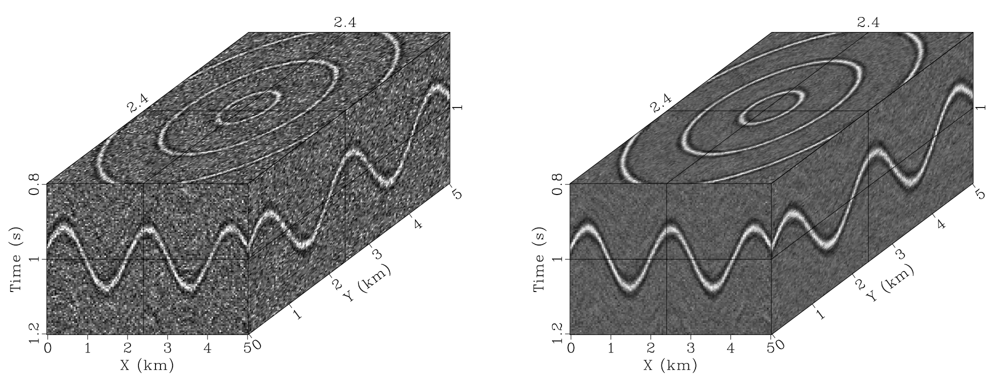

Figure 4: The results of f-x NRNA (a) and f-x-y NRNA (b). $\boxed{\text{rna3d/sin tpre2d,tpre}}$

SYNTHETIC EXAMPLES

We demonstrate the effectiveness of the proposed *f*-*x*-*y* NRNA using two synthetic dataset. The first synthetic example involves only one curved surface. Fig. 2(a) shows the synthetic dataset. Three slices of Fig. 2(a) illustrate the Y=2.4 km, X=2.4 km and Time=1 s, respectively. The following figures in this paper have the same way for display. The traveltime of this surface is shifted sine function (Fig. 3(a)). We can find that the traveltime is not linear varying. Therefore, we cannot use stationary *f*-*x*-*y* prediction filtering to estimate the effective signal. Fig. 5(b) is the noisy data. This curved surface event is greatly contaminated by random noise. We respectively use *f*-*x* NRNA and f-x-y NRNA to attenuate the random noise and compare their results (Fig. 5(c)- 5(d)). The SNRs of *f*-*x* NRNA and *f*-*x*-*y* NRNA are 0.34 and 2.4, respectively. Although f-x NRNA has suppressed a lot of random noise, there are still some random noises in the result (Fig. 5(c)). Compared with *f*-*x* NRNA, *f*-*x*-*y* NRNA gives a better result. The curved surface event is very clear and consistent, which may be easier to automatic event tracking for interpretation. Fig. 3(b) shows the imaginary part of *f*-*x*-*y* NRNA coefficients at a given shift $a_{x,y,i_0}(f)$, which are smooth along with space axes. From the slice with 20.833 Hz (up slice in Fig. 3(b)), one can find that the coefficients reflect the information of traveltime or time shifts between circumjacent traces (Fig. 3(a)). From the frontal and lateral slices in Fig. 3(b), one can conclude that the coefficients are related to dips of events from the frontal and lateral slices in Fig. 2(a). The coefficient is zero if the event is horizontal (e.g. position B). The coefficients are respectively positive and negative if the events are upgoing (e.g. position A) and downgoing (e.g. position C). The estimated rusult of coefficients is consistent with theoretical analysis.

The second synthetic example is a synthetic shot gather with four hyperbolic events (Fig. 5(a)). Here, we consider anisotropy of the propagating velocity, so that there are intersecting events in Y slice but they are not intersecting in X slice (the second and third events). Comparing the results of *f*-*x* NRNA (Fig 5(c)) and *f*-*x*-*y* NRNA (Fig 5(d)), we can find that *f*-*x*-*y* RNA can remove more noise that *f*-*x* NRNA, especially for poor signals (for example, far offset of the events indicated by arrows in Fig. 5(a)- 5(d)). The SNRs of *f*-*x* NRNA and *f*-*x*-*y* NRNA are 0.95 and 2.61, respectively. Both of these synthetic examples demonstrate the proposed *f*-*x*-*y* NRNA can be effectively use to attenuation random noise for 3D seismic data cube.

APPLICATION ON FIELD POSTSTACK DATA

The *f*-*x*-*y* NRNA method is applied to a 3D image after time migration (Fig. 6). The shallow structures are simple plane layers (above 1 s) and the deep structures are complex curved layers (below 1 s). We respectively apply *f*-*x* NRNA and *f*-*x*-*y* NRNA to enhance the reflectors of this 3D image cube. Fig. 7 shows the imaginary part of *f*-*x*-*y* NRNA coefficients at a given shift $a_{x,y,i_0}(f)$. Similar to synthetic example, the *f*-*x*-*y* NRNA coefficients are smooth and reflect the information of event dips. In

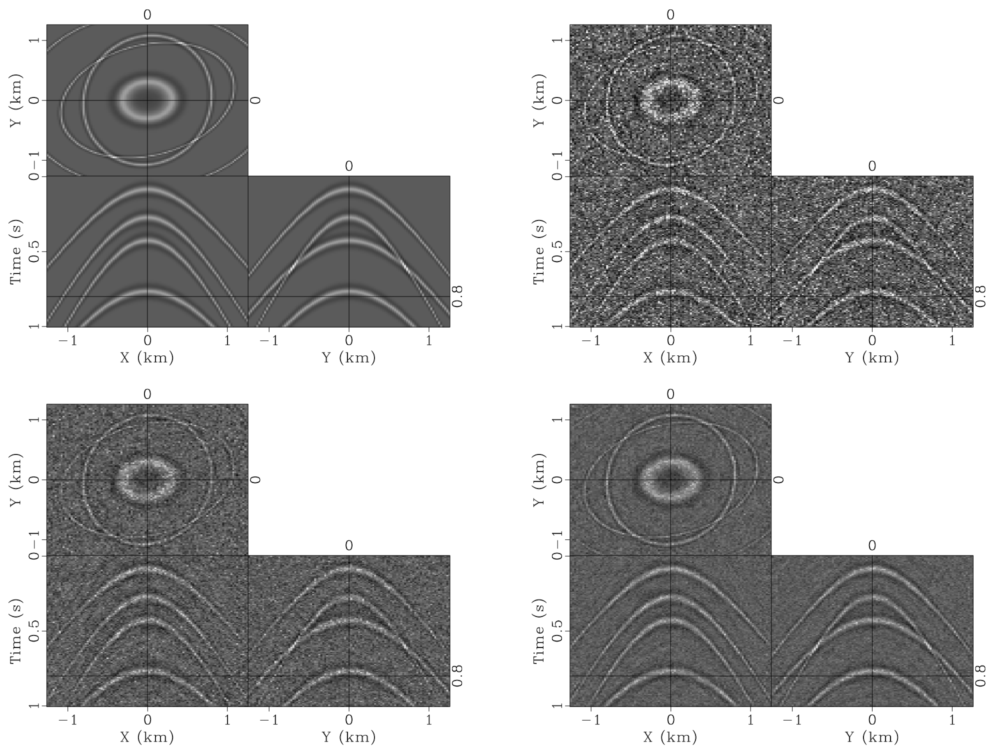

Figure 5: (a) Synthetic 3D shot gather. (b) Noisy data. (c) The result of f-x RNA. (d) The result of f-x-y RNA. rna3d/shot cmp0,cmp,tpre2d,tpre

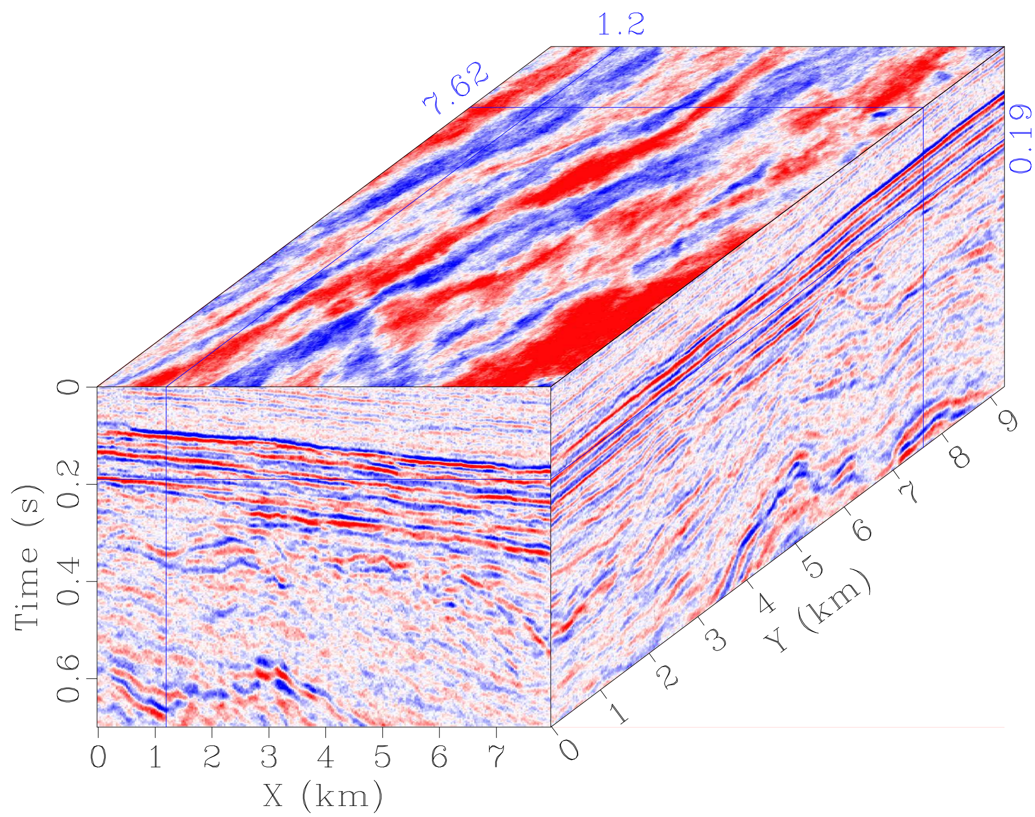

Figure 6: The 3D field data cube after time migration. rna3d/real data

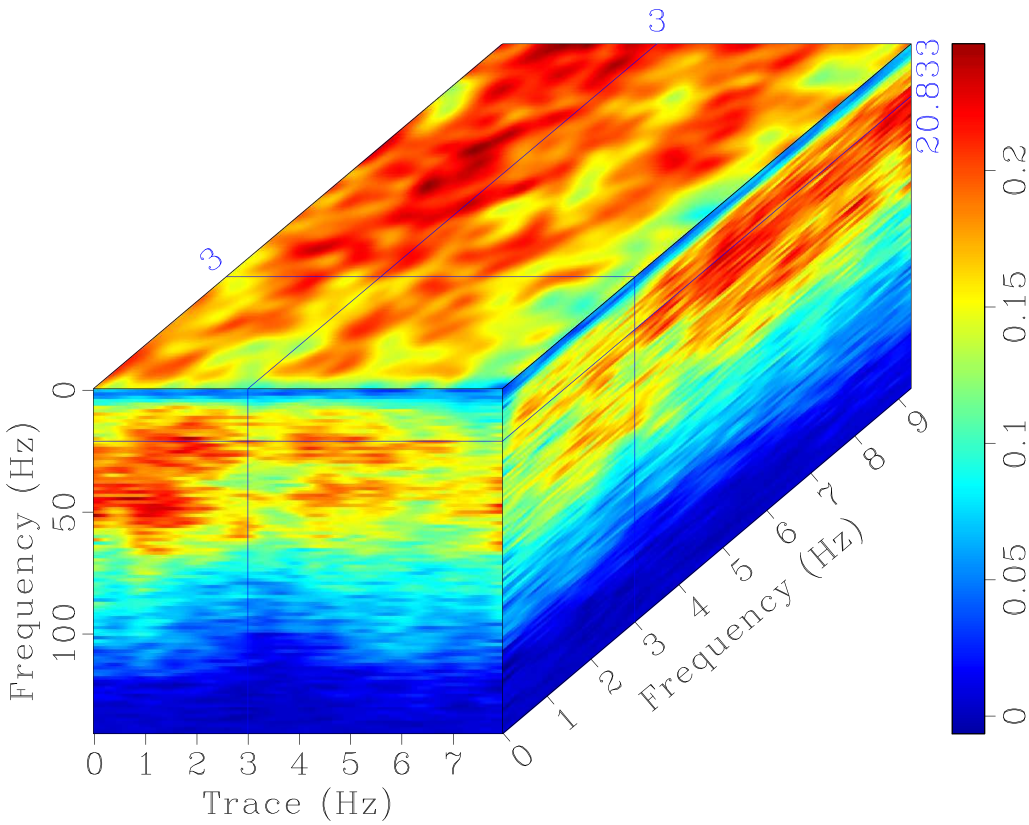

Figure 7: The imaginary part of f-x-y NRNA coefficients at a given shift $a_{x,y,i_0}(f)$ for real dataset. rna3d/real flt-np

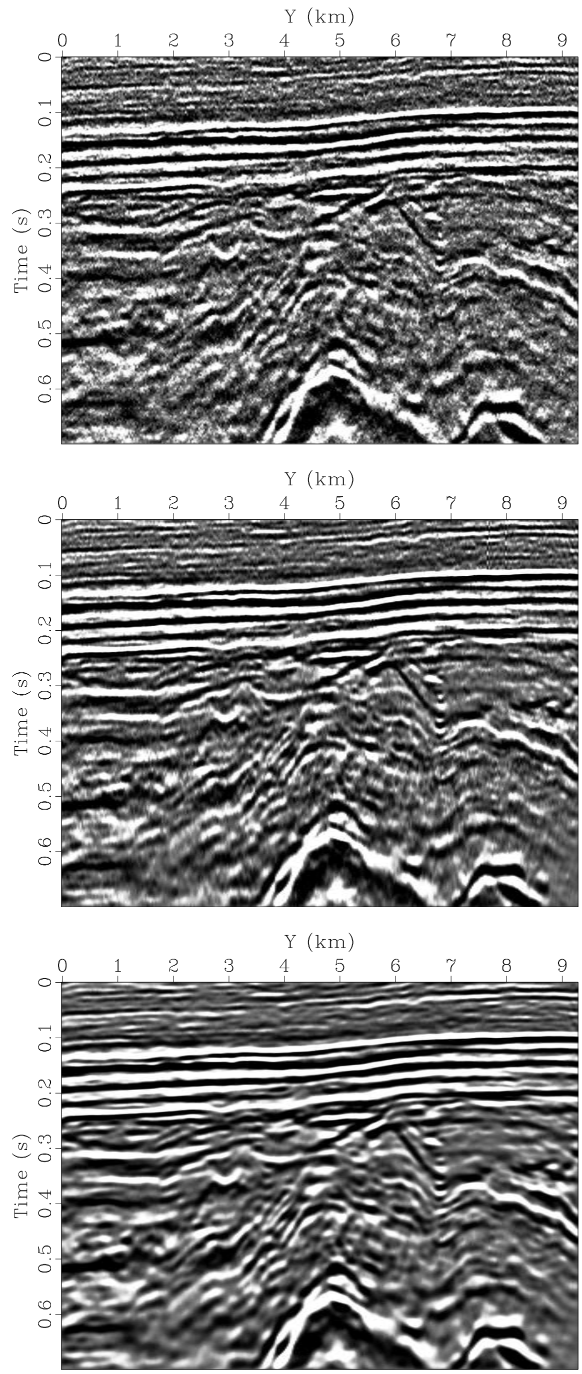

Figure 8: The slice X of field data cube. (a) Original data; (b) *f*-*x* NRNA; (c) *f*-*x*-*y* NRNA. rna3d/real wi,wi-2,wi-3

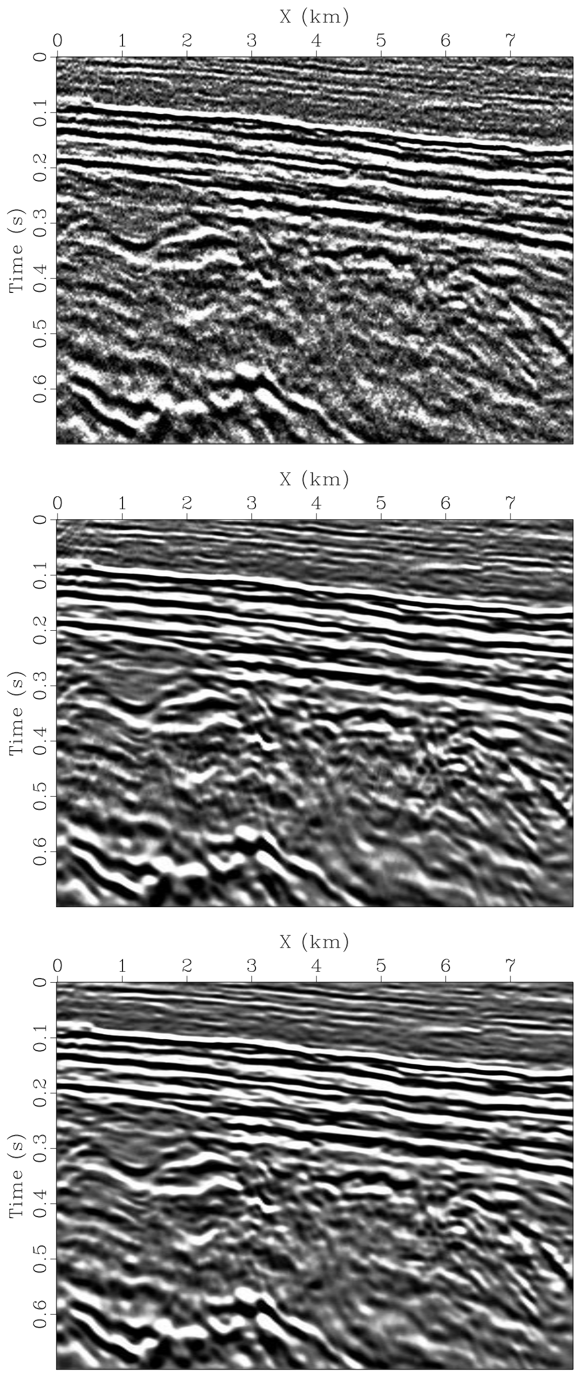

Figure 9: The slice Y of field data cube. (a) Original data; (b) *f*-*x* NRNA; (c) *f*-*x*-*y* NRNA. rna3d/real wc,wc-2,wc-3

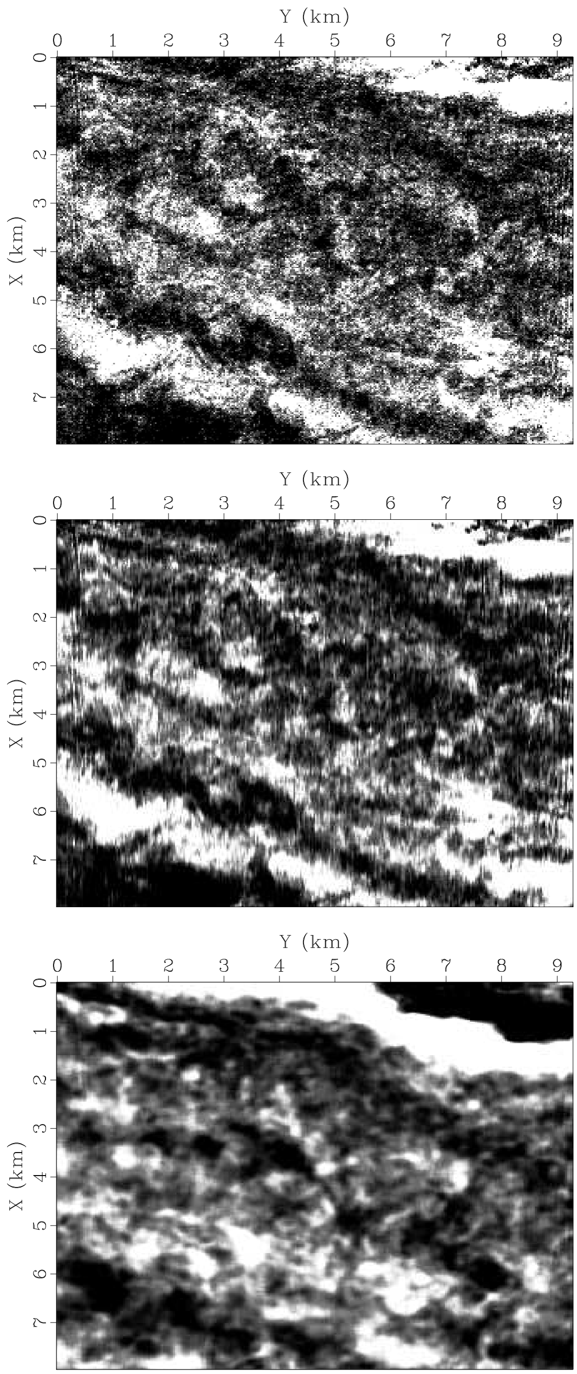

Figure 10: The time slice of field data cube. (a) Original data; (b) *f*-*x* NRNA; (c) *f*-*x*-*y* NRNA. rna3d/real wt,wt-2,wt-3

this example, we use M=2 for f-x-y NRNA and M=8 for f-x NRNA, respectively. Figs. 8(a)- 8(c) and 9(a)- 9(c) respectively shows the X and Y slices after f-x NRNA noise attenuation and f-x-y NRNA noise attenuation. We can find that f-x-y NRNA method can give a better result than f-x NRNA method. The result of f-x-y NRNA has a much better lateral continuity. These two methods not only improve the shallow plane events evidently (e.g. 0s -0.5s), but also improve the deep curved surface events (e.g. the area indicated by ellipse). This is because these two methods both are nonstationary methods, which is suitable for curved events. In addition, comparing f-x NRNA and f-x-y NRNA methods from time slices (Fig. 10(a)- 10(c)), one can also see that the f-x-y NRNA gives more consistent result. The lateral continuity and trace-by-trace consistency of the reflections are crucial in structural interpretation of seismic data by reflection picking especially for the auto-picking tools of interactive interpretation systems (Fomel, 2010).

CONCLUSIONS

We have proposed a novel method for seismic noise attenuation using f-x-y NRNA for 3D seismic data. f-x-y NRNA is the 3D extension of f-x NRNA. By using more information to predict the seismic signal, the f-x-y NRNA improves the denoising result for 3D seismic data. The varying coefficients of the f-x-y NRNA are smooth along space coordinates for a given direction. The smoothness is controlled by shaping regularization, which has the key parameter: the smooth radius. The smooth radius can be selected by user according to the smoothness of assumed coefficients. This approach does not require breaking the input data into local windows along space axis, although it is conceptually analogous to sliding spatial windows with maximum overlap. Execution time of f-x-y NRNA is reduced by iteration inversion and shaping regularization. Synthetic and field data examples both confirm that the proposed f-x-y RNA approach can be significantly more effective in noise attenuation and consistency improvement than f-x RNA for 3D seismic data. Therefore, it may be useful in conjunction with interactive interpretation systems and auto-picking tools such as automatic event tracking.

ACKNOWLEDGMENTS

We would like to thank Yang Liu and Jingye Li for inspiring discussions. This research was partially supported by Science Foundation of China University of Petroleum, Beijing (No. YJRC-2013-39) and the National Natural Science Foundation of China (no. U1262207).

REFERENCES

Abma, R., and J. Claerbout, 1995, Lateral prediction for noise attenuation by t-x and f-x techniques: Geophysics, **60**, 1187–1896.

Canales, L., 1984, Random noise reduction: 54th Annual International Meeting, Soc. of Expl. Geophys., 525–527.

Chase, M., 1992, Random noise reduction by fxy prediction filtering: Exploration Geophysics, **23**, 51–56.

Fomel, S., 2007, Shaping regularization in geophysical-estimation problems: Geophysics, **72**, R29–R36.

———, 2009, Adaptive multiple subtraction using regularized nonstationary regression: Geophysics, **74**, V25–V33.

———, 2010, Predictive painting of 3d seismic volumes: Geophysics, **75**, A25–A30.

Galbraith, M., 1984, Random noise attenuation by f-x prediction: 61th Annual International Meeting, Soc. of Expl. Geophys., 14281431.

Gulunay, N., 1986, Fxdecon and complex wiener prediction filter: 56th Annual International Meeting, Soc. of Expl. Geophys., 279–281.

———, 2000, Noncausal spatial prediction filtering for random noise reduction on 3-d poststack data: Geophysics, **65**, 1641–1653.

Gulunay, N., V. Sudhakar, C. Gerrard, and D. Monk, 1993, Prediction filtering for 3-d poststack data: 63rd Annual International Meeting, Soc. of Expl. Geophys., 11831186.

Hodgson, L., D. Whitcombe, S. Lancaster, and P. Lecocq, 2002, Frequency slice filtering - a novel method of seismic noise attenuation: 72th Annual International Meeting, Soc. of Expl. Geophys., 2214–2218.

Hornbostel, S., 1991, Spatial prediction filtering in the t-x and f-x domains: Geophysics, **56**, 2019–2026.

Liu, G., X. Chen, J. Du, and K. Wu, 1991, Random noise attenuation using f-x regularized nonstationary autoregression: Geophysics, **56**, 2019–2026.

Liu, G., X. Chen, and J. Li, 2009, Noncausal spatial prediction filtering based on an arma model: Applied Geophysics, **6**, 122–128.

Liu, Y., and S. Fomel, 2011, Seismic data interpolation beyond aliasing using regularized nonstationary autoregression: Geophysics, **76**, V69–V77.

Ma, J., and G. Plonka, 2010, The curvelet transform: IEEE Signal Processing Magazine, **27**, 118–133.

Naghizadeh, M., and M. Sacchi, 2009, f-x adaptive seismic-trace interpolation: Geophysics, **74**, V9–V16.

Ozdemir, A., A. Ozbek, R. Ferber, and K. Zerouk, 1999, F-xy projection filtering using helical transformation: 69th Annual International Meeting, Soc. of Expl. Geophys., 1231–1234.

Sacchi, M., and H. Kuehl, 2001, Arma formulation of fx prediction error filters and projection filters: Journal of Seismic Exploration, **9**, 185–197.

Spitz, S., 1991, Seismic trace interpolation in the f-x domai: Geophysics, **56**, 785794.

Tang, G., and J. Ma, 1991, Applications of total variation based curvelet shrinkage for three-dimensional seismic denoising: IEEE Geoscience and Remote Sensing Letters, **8**, 103–107.

Wang, W., and G. West, 1991, F-x filters with dip rejection: 61st Annual International Meeting, Soc. of Expl. Geophys., 14361438.

Wang, Y., 2002, Seismic trace interpolation in the f-x-y domain: Geophysics, **67**, 1232–1239.